528743

AIAA 2001-2236
Measurements and Predictions for a Distributed Exhaust Nozzle

K.W. Kinzie and M.C. Brown
NASA Langley Research Center

D.B. Schein and W.D. Solomon, Jr.
Northrop Grumman Corporation

7th AIAA/CEAS Aeroacoustic Conference
28-30 May 2001
The Maastricht Exhibition and Congress Centre
Maastricht, The Netherlands

Measurements and Predictions for a Distributed Exhaust Nozzle

Kevin W. Kinzie* and Martha C. Brown
NASA Langley Research Center, MS 166
Hampton, VA 23681

David B. Schein and W. David Solomon, Jr.**
Northrop Grumman Corporation
Integrated Systems Sector, Air Combat Systems
El Segundo, CA 90245-2804

Abstract

The acoustic and aerodynamic performance characteristics of a distributed exhaust nozzle (DEN) design concept were evaluated experimentally and analytically with the purpose of developing a design methodology for developing future DEN technology. Aerodynamic and acoustic measurements were made to evaluate the DEN performance and the CFD design tool. While the CFD approach did provide an excellent prediction of the flowfield and aerodynamic performance characteristics of the DEN and 2D reference nozzle, the measured acoustic suppression potential of this particular DEN was low. The measurements and predictions indicated that the mini-exhaust jets comprising the distributed exhaust coalesced back into a single stream jet very shortly after leaving the nozzles. Even so, the database provided here will be useful for future distributed exhaust designs with greater noise reduction and aerodynamic performance potential.

Introduction

Jet noise continues to be a dominant noise source during takeoff of commercial aircraft. Recent advances in jet noise reduction have focused on changes in the engine cycle, increased bypass ratio, or mixing enhancement devices. While these techniques are incrementally improving the community noise situation, revolutionary improvements in conventional engine/airframe systems are required to meet the NASA noise reduction goal of 20 dB in 25 years. One such concept with potential to make significant progress toward the 25-year goal is a distributed exhaust nozzle. The benefit of the distributed exhaust relies on expanding the engine air through many small nozzles rather than one or two large nozzles. The beneficial aeroacoustic properties of the small nozzles result in perceived community noise reduction. One such distributed exhaust nozzle showed up to 25 dB jet noise suppression[1]. However, thrust losses were high for this type of design.

Noise suppression from the distributed exhaust nozzle concept results from a favorable shift in the spectral shape of the radiated jet noise. The smaller jets radiate noise at significantly higher frequencies compared to larger jets. Atmospheric attenuation increases nearly exponentially with increasing frequency and noise components contribute less and less to the FAA EPNL noise metric as the frequency increases above 4 kHz. In fact, noise produced at frequencies higher than 10 kHz is not even included in the calculation of EPNL. In addition to shifting the noise signature toward potentially more favorable high frequencies, the small jets mix more rapidly with the ambient air and reduce the speed and temperature of the jet plume to lower levels that, in turn, reduce the radiated noise.

Traditionally, distributed exhaust nozzle concepts have been studied from the perspective of replacing conventional engine exhaust nozzles with another configuration composed of many small tubes, chutes, or spokes. However, this inevitably leads to high levels of base drag due to the aft facing area required to distribute the exhaust. NASA Langley is pursuing research aimed at studying the distributed exhaust concept from an integrated exhaust/airframe system perspective where the propulsion system is integrated into the airframe and the small exhaust nozzles are distributed over large portions of the wing surface area. An integrated distributed exhaust propulsion system has even greater potential for noise reduction than the isolated nozzle component

---

* Senior Member, AIAA
** Member, AIAA

referenced previously since additional noise suppression will be realized through shielding of engine noise away from the community by the airframe design.

As part of the Advanced Vehicle System Technology base program, the Jet Noise Laboratory (JNL) at LaRC and Northrop Grumman Corporation (NGC) have been investigating distributed exhaust nozzle (DEN) concepts in an attempt to achieve noise reduction while minimizing performance loss. The configuration tested was chosen from a number of Northrop Grumman designs, and was selected based on ease of manufacture and budget constraints. This geometry represented that with the highest predicted thrust performance. However, this design did not have the greatest potential for reduction of jet mixing noise among all of the preliminary designs. Hence, a primary objective of this effort was to demonstrate that Northrop Grumman's CFD approach could accurately predict the propulsive performance details of such a complicated exhaust geometry, validating its utility as a design tool for more aggressive noise suppressing DEN configurations in the future. The candidate design was tested in Langley's Low Speed Anechoic Wind Tunnel (LSAWT). Acoustics and thrust performance were measured along with total pressure and temperature plume surveys. This paper will describe the nozzle CFD analysis and test results.

Nozzle Description

The distributed exhaust nozzle was comprised of an array of small, high aspect ratio rectangular shaped nozzles as show in Fig. 1a. The nozzle flowpaths were formed by the surfaces of airfoil shaped slats (Fig. 1b) stacked on top of one another and staggered in the axial direction. The total design exit area of the DEN analyzed in CFD was 40.8 in^2. The total exit area of the wind tunnel model was computed by summing the exit area of each mini-nozzle and was 42.4 in^2. In order to assess the noise characteristics of the DEN, two reference nozzles were tested at the same cycle conditions. The first was a conical nozzle with an exit area of 39.4 in^2 and will be referred to as the 1D reference nozzle. The second was a rectangular nozzle with an aspect ratio of 2.1 and an exit area of 39.6 in^2 and will be referred to as the 2D reference nozzle. The DEN was sized with a slightly larger design exit area (3%) compared to the 2D reference nozzle so that the two nozzles would have approximately the same mass flow based upon the CFD prediction. As will be seen from the measurements, even though the aspect ratio of the DEN base area is approximately 1, the flowfield quickly evolves into a plume with an aspect ratio very similar to that from the 2D reference nozzle, making comparisons to that nozzle particularly relevant. All length scales reported here are normalized by the equivalent diameter, D_{eq}, of the respective nozzle where D_{eq} is equal to the diameter of a circular nozzle with the same exit area.

CFD Analysis

Prior to the test, extensive CFD analysis was performed using Northrop Grumman's Generalized Compressible Navier-Stokes (GCNS) code with the primary objective of obtaining net thrust estimates. GCNS solves the thin layer Reynolds-averaged Navier-Stokes equations for ideal air on structured patched or overset grid topologies. The equations are expressions of rate-based conservation of mass, momentum, and energy at a given point in time. Time and space derivatives are treated sequentially rather than simultaneously. A node-based finite volume approach to space derivatives facilitates conservation within a given grid block. Equations are solved using a diagonalized Beam-Warming implicit approximate-factorization method. Central differencing is applied to advective terms with scalar artificial dissipation (a Jameson Schmidt Turkel scheme). A ratio of specific heats of 1.4 was assumed because the GCNS code does not currently support variable specific heats.

Mentor's k-ε / k-ω Shear Stress Transport (SST) turbulence model was used for all runs[2]. Turbulent flow was assumed on all surfaces except near the internal upstream charging station. Each case was first run with at least one level of grid sequencing with constant CFL scaling. More often than not, the large variation in off-surface grid cell volumes resulted in a non-physical waviness in the plumes which was eliminated by resuming the run with a limited maximum time step (no greater than the smallest maximum time step of all blocks). Thus a steady state solution was used to pre-condition a pseudo-time accurate run on the fine mesh.

The grid for the 2-D reference nozzle consisted of 14 overset grid blocks and 4,099,926 points for the quarter modeled, which included the fan flow / core flow splitter and the charging station rakes. For the results presented here, these flows had matching total pressure and total temperature. The grid extends 200 equivalent diameters downstream and 100 radially. The run for the 2-D reference nozzle required 15.45 processor days on NGC's Hewlett Packard SPP 2000 Exemplar. Wall-clock time was about 23 hours.

Due to computer memory limitations, the DEN case was run in two phases. The initial grid contained 174 overset blocks and 17,975,730 points. It included the same components as the 2-D reference nozzle (splitter, rakes, etc.) but a somewhat coarser plume grid. Thrust estimates were obtained after running this grid

64.58 processor-days (4 wall-clock days) single-precision. Total memory required with one level of grid sequencing was 2.76 gigabytes.

The grid blocks upstream of the internal transition duct exit were then removed, and the resolution of the plume blocks was increased for comparison with the JNL plume study data. The new grid was initialized with the old solution, with the conditions fixed at the internal transition duct exit. This new grid consisted of 164 grid blocks and 17,645,460 points. An additional 5900 pseudo-time accurate iterations were run for 56.18 more processor-days (with 11.74 spent on writing output files) to resolve the plume and to simultaneously investigate the existence of unsteady flow.

Experimental Approach

Tests of the design were performed in the Low Speed Aeroacoustic Wind Tunnel in NASA Langley's Jet Noise Lab. Figure 2 shows the DEN installed on the jet engine simulator (JES) in the wind tunnel. The JES is a dual stream propulsion system with two independently controlled air streams that can each provide up to 15 lbm/s at temperatures up to 2000° R from propane burners located in each leg. For the results reported in this paper, each stream was operated at the same pressure and temperature and mixed together in a common plenum section upstream of the DEN. The LSAWT is capable of simulating forward flight Mach numbers up to 0.32 by surrounding the JES with flow through the 56.4" square LSAWT test section. All of the tests reported in the paper were performed with free jet Mach number of 0.1.

A 28 element linear microphone array located at a distance of 12 ft. from the nozzle centerline was used to acquire the acoustic data. The nozzle was rotated to obtain noise measurements at various azimuthal orientations. Figure 3 shows the nozzle orientation for the DEN and 2D reference nozzle at azimuthal angles of 0° and 90° reported in this paper. For both the DEN and 2D reference nozzle, measurements in the 0° azimuthal orientation are referred to as major axis plane measurements and measurements in the 90° azimuthal orientation are referred to as minor axis plane measurements. The microphones were ¼" diameter, operated with the grid caps removed, and calibrated with a pistonphone and electrostatic calibrator before and after the test. The microphone data reported here are shown on a 1 ft. arc around the nozzle exit and have had atmospheric propagation effects removed based upon the local test day conditions. The data are also presented at model scale. Scaling DEN acoustic data to full size is problematic since the size of the mini-nozzles is already approximately full scale, while the overall exit area is not. Therefore, a scale factor based on overall jet area would also incorrectly shift the high frequencies associated with the mini-jets. Rather than attempting to account for the two different length scales in the data analysis, the data are left at model scale. Since all three test nozzles have very similar exit areas, evaluating the data at model scale is considered sufficient for the one-third octave band analysis presented here.

For the aerodynamic performance measurements, separate choked venturi flow meters were used to measure the air mass flow through each leg of the JES and turbine flow meters were used to measure the fuel flow burned in the combustors. Thrust produced by the nozzle was measured using the six-component thrust balance system that is a part of the JES.

Flow field measurements were made separately from acoustic measurements by a motorized traverse system that controlled a rake comprised of three total pressure elements and three total temperature elements. By traversing the rake, total temperature and pressure measurements were made at identical locations so that Mach number and velocity could be derived assuming that the local static pressure was equal to ambient. This is a valid assumption except for very close to the DEN exit.

Data were acquired for each nozzle at the test conditions shown in Table I. Even though the JES can be operated with different conditions in the fan and core stream, both streams were set with the same temperature and pressure for the results reported here. The nozzle pressure ratio (NPR) and total temperature conditions (T_t) in Table I were derived by starting with the separate flow turbofan exhaust system cycle line that was used during the Separate Flow Nozzle Test at Glenn Research Center[3] and fully mixing the fan and core streams together to obtain the points in Table I. Unless otherwise noted, all of the data presented in this paper correspond to test point 13 which is typical of take-off power condition.

Flowfield Measurements and Predictions

Figure 4 shows measured and predicted centerline velocity distributions for the DEN and the 2D reference nozzle for test point 13. Due to the irregular exit geometry of the DEN, the origin is taken to be at the axial station of the 2D exit plane so that both nozzles are referenced to the same axial location. This point on the DEN is approximately halfway between the exit planes of the first mini-nozzle and the most aft mini-nozzle. The potential core of the DEN is less than $2D_{eq}$ shorter than the 2D reference nozzle indicating that the mixing from the two nozzles is similar. The

CFD slightly overpredicts the length of the potential core region, but does a good job simulating the axial decay of both jets. Figure 5 shows CFD predicted contour plots of Mach number for the DEN and the 2D jet in both the minor and major axis planes. As evidenced in the centerline velocity distribution plots, the DEN has a slightly shorter and generally smaller potential core region, but the overall plume dimensions and characteristics are not dramatically different than those of the 2D reference nozzle.

Figure 6 shows the measured total pressure over one nozzle quadrant just downstream of the most aft slot trailing edge. At this location (x/D_{eq} = 0.14), only the last two individual slot jets can be identified. The large pressure deficit visible at approximately y/D_{eq} = 0.3 is due to the wake from a structural gusset required to hold the small airfoil slats in place (see Fig. 1a). Figure 7 shows measured and predicted velocity profiles in the minor axis of the DEN and 2D jets at an axial location close to the nozzle exits and also a location further downstream. The DEN is shown at x/D_{eq} = 2.65 and 8.84 and the 2D at 3.10 and 9.30. Unfortunately, measurements were not made at the same nondimensional location for each jet. However, the displayed locations are close and still provide a good picture of the plume development. The CFD does a good job predicting the velocity profile for both jets. As expected from the exit pressure plane data of Fig. 6, there is no evidence of the individual mini-jets in the DEN profiles and it appears that the small jets have quickly coalesced into a single plume. Figure 8 shows the shear layer thickness, h, of the 2D and DEN jets as derived from the experimental velocity profiles. The growth rates of the two jets are very similar with the DEN even having a slightly lower growth rate than the 2D jet. All of these measurements indicate that the mixing characteristics of the DEN are not substantially different from those of the 2D reference nozzle.

For substantial noise reduction, it is important that the individual jets retain their identity long enough to increase the mixing and shift the radiated noise to higher frequency. However, the flowfield data do not show jet-to-jet mixing taking place. A final piece of evidence to support this conclusion is seen in the CFD predictions of velocity and turbulent kinetic energy shown in Figs. 9 and 10, respectively. The velocity prediction shown in Fig. 9 does not indicate significant mixing between the individual jets. In Fig. 10, high levels of turbulent kinetic energy (TKE) are seen in the shear layer at the outer edge of the jet, but the TKE in the vicinity of the mini-nozzles is very low, also indicating that there is little mixing taking place between the small jets. The airfoil shapes were designed for low drag, but their close proximity and efficiency produces jets that coalesce into a larger plume resembling that of the 2D reference nozzle more than a distributed exhaust with small discrete jets.

Aerodynamic Performance

The most challenging aspect of a DEN design is maintaining sufficient flow and thrust performance so that the nozzle is a viable alternative to traditional exhaust systems. As with most noise reduction strategies, the mechanisms that provide low noise are typically at cross purposes with those that produce high thrust values. The very nature of spreading out the exhaust plume typically results in large base area drag and the associated high nozzle surface areas result in low discharge coefficients. A major objective of this research program was to use the CFD to design a DEN with a reasonably high thrust and discharge coefficient and to show that the CFD could accurately predict these values.

The discharge coefficient, C_d, is important because it is used to size the nozzle for efficient air mass flow set by an engine's turbomachinery. For this paper, the discharge coefficient is defined as the actual measured or predicted mass flow normalized by the ideal 1D mass flow through the nozzle exit. Figure 11 shows the measured and predicted discharge coefficient from the DEN and the 2D reference nozzle. During the test program, the DEN was rotated to obtain noise measurements at various azimuthal angles relative to the nozzle. Thrust performance data were also collected at each of these rotation angles and are shown collectively in Fig. 11. While small changes in the performance characteristics might be expected due to the effects of rotating the nozzle relative to the JES strut, the wind tunnel exit, and fixed internal rig mountings, the multiple measurements do provide some degree of repeatability. The multiple measurements for the 2D reference nozzle represent repeat data points. It is seen that the measured C_d is repeatable at each nozzle pressure ratio within about +/- 0.3%. Compared to the 2D reference nozzle, the DEN C_d is 3-5% lower over the NPR range. At the common nozzle pressure, CFD predicts about a 3% lower C_d for the DEN, while the test results show about a 4% deficit.

Figure 12 shows the same comparison for the thrust coefficient measurement and prediction. The thrust coefficient, C_{fg}, is defined as the measured axial thrust normalized by the ideal 1D thrust which is proportional to the actual mass flow and ideally expanded nozzle exit velocity. Again, multiple measurements are shown representing each of the nozzle azimuthal rotations. The accuracy of the thrust measurements is estimated to be approximately +/- 1.5%. Again, the CFD predictions are very close to the measured values and fall within the measurement error

range. The DEN C_{fg} is lower than the 2D reference by a value of approximately 5%. While significant improvements in the thrust performance are required for a viable nozzle system, the ability of the CFD to predict the C_{fg} is encouraging. It is also possible that for some military applications or for nonconventional DEN installations, such as in a truly distributed propulsion system with mini-exhausts over a whole wing surface, that lower performance levels could be tolerated if there were other system benefits such as reduced weight or upper surface blowing effects.

Noise Measurements

With a good grasp of the flowfield characteristics of the DEN, the acoustic measurements can be evaluated and interpreted in light of the implications of the flowfield data. Figures 13 and 14 show the overall sound pressure level (OASPL) directivity for the DEN and the 1D and 2D reference nozzles at azimuthal orientations of 0° and 90°. In the 90° orientation, the microphones are aimed at the short dimension of the DEN and 2D reference nozzle and are perpendicular to the trailing edge of the airfoil slats as shown in Fig. 3. In the 0° orientation, the microphones are aimed at the long dimension of the DEN and 2D reference nozzle and are aligned with the trailing edge of the airfoil slats as show in Fig 3. Measurements at other angles were taken for the DEN, but are not shown here as they do not add significantly to the data interpretation. Also, recall that the data presented are normalized to an arc of 1 ft radius with all atmospheric propagation effects removed.

It is immediately clear that this DEN design did not achieve significant levels of noise reduction. In fact at many angles, the DEN is 2-4 dB louder than either the 1D or 2D reference nozzle. On the 0° axis, the DEN is generally quieter than the 1D reference nozzle, except at the most forward angle locations. The DEN is quieter than the 2D reference nozzle by 1-2 dB at polar angles above 130°. Between polar angles of 90° to 130°, the DEN is slightly louder than the 2D reference nozzle but becomes 2-3 dB louder than the 2D reference nozzle further toward the forward quadrant. For the 90° orientation, the DEN is louder than either reference nozzle over the entire directivity range except for at the very most aft quadrant angles. While it was hoped that the acoustic performance of the DEN would be better, examination of the flowfield data and the noise spectra reveal the shortcomings of this DEN design as an acoustic suppression system.

Recall from the flowfield data that the plume of the DEN was not significantly different than that of the 2D reference nozzle. There was little mixing between the individual jets and the identities of the mini-jets were not maintained as they quickly coalesced into a single jet plume with characteristics of the 2D reference jet plume. The growth rates and individual velocity profile distributions were similar and as a result, the noise characteristics of the DEN are also similar to the 2D reference nozzle with little noise suppression. It is interesting that the DEN actually increased the noise over a wide range of the directivity. This unexpected trend can be explained by looking at the noise spectra at several directivity angles.

The greatest increase in radiated noise by the DEN is observed in the forward quadrant. Those angles will be examined first. Figures 15 and 16 show one-third octave spectra computed from narrowband data from the DEN and the 1D and 2D reference nozzles measured at a polar angle of 50° from the jet axis for the 0° and 90° azimuthal orientations. Both spectra show very high noise levels from the DEN in the 3-5 kHz range with levels 5-8 dB above either of the reference nozzles. These peaks dominate the OASPL levels at many of the forward angles. While additional spectra are not shown here, a very interesting characteristic of this noise source is that starting in the forward quadrant, the peak noise frequency increases as the observer moves towards the sideline polar angle location of 90°. This is characteristic of a convecting noise source with a Doppler frequency shift. The Doppler shifted frequency, f_d, is defined as $f_d = f(1 - M_c\cos\theta)$ where f is the measured frequency, M_c is the convection Mach number of the moving source, and θ is the observer angle relative to the jet axis. While the noise source is 1-2 kHz wide, an attempt was made to identify the peak frequency at every polar angle where the source could be identified in the narrow band data. The open symbols in Fig. 17 show the peak frequency as a function of downstream angle for three different pressure ratios. For each NPR, the peak frequency monotonically increases from a polar angle of 43 degrees up to an angle of 75 degrees. Each of these measured frequencies was then normalized by the Doppler factor of $(1 - M_c\cos\theta)$ where M_c was chosen such that it minimized the variation of the Doppler shifted frequency, f_d, over the entire measured polar range. These inferred Doppler shifted frequencies are shown by the closed symbols in Fig. 17. For all three angles, approximately the same inferred value of M_c = 0.49 gave the minimum variation of f_d shown in Fig. 17. This is very strong evidence that the noise source producing the extraneous sound in the 3-5 kHz range is being convected downstream by the jet at a convection Mach number just under half of the jet speed. Furthermore, data not shown here indicate that this convection Mach number is independent of the free jet velocity implying that the noise source is embedded well within the core of the jet where it is unaffected by

the free stream flow. The exact noise source mechanism was not identified in this study, but it is hypothesized that a turbulence source is being generated in a constructive manner by the very regular array of airfoil slots and convected downstream while radiating noise to the far-field.

Another strong noise source is seen in the spectra of Figs. 15 and 16 in the frequency bands above 30 kHz up to the maximum one-third octave frequency band of 80 kHz. Since this noise source is most prevalent at the 90° orientation, it was hypothesized that this noise was generated by trailing edge noise from the small airfoils that comprise the mini-nozzles. This type of noise would peak in the direction perpendicular to the surface of the airfoils as seen here. To evaluate this hypothesis, the airfoil self-noise prediction code of Brooks et al.[4] was exercised using the geometry and flow conditions around an individual airfoil in the DEN. Trailing edge noise phenomena are best evaluated at directions perpendicular to the airfoil surface so the measured acoustic spectrum at a polar angle of 90° and an azimuthal angle of 90° for the DEN is shown in Fig. 18. In addition to the measured DEN spectrum, predictions from the airfoil self-noise code are also shown in Fig. 18. Predictions for a single airfoil and for an array of 12 airfoils are included. The predictions match the frequency range of the measured DEN spectra and also bracket the amplitude of the DEN spectra. Since all twelve DEN airfoils exposed to the microphones would not be radiating to the 90° polar microphone with maximum efficiency, it is reasonable to expect the measured DEN data to fall between the predictions of a single airfoil and twelve airfoils. Therefore, the predictions indicate that the small airfoils have the potential for noise radiation consistent in frequency and amplitude of that observed in the DEN spectra.

While the code predicts the noise from five different airfoil noise sources, it does not predict whether or not these components are actually present on a given airfoil. The component predictions in the code indicate that the dominant potential airfoil noise source is due to trailing edge bluntness vortex shedding which peaks narrowly in the 63 kHz octave band. The broadening of the predicted spectra in the higher frequency bands is contributed by laminar boundary layer vortex shedding noise. Other noise components made negligible contribution to the predicted noise. Based upon the blunt trailing edge of the airfoil geometry seen in Fig. 1b, it is highly likely that the peak frequency seen in the DEN spectra in the 63 kHz octave band is a result of trailing edge bluntness vortex shedding. It is also possible that the broadening of the DEN spectra is due to laminar boundary layer vortex shedding, however no measurements were made that would indicate whether the airfoils had turbulent or laminar boundary layers. In any case, this is very compelling evidence that the source of the high frequency DEN noise is actually a result of the airfoil trailing edge noise characteristics of the small airfoil slats.

It is at this point that the scaling issues for the DEN become important. The model scale size of the airfoils and mini-nozzles is close to what they would be in an actual full-scale application. Of course, there would be many more of them. Therefore, since this high frequency source is associated with the airfoil geometry, the frequency range would not scale down and the airfoils would still generate noise in the 30-80 kHz at full scale. Noise in this frequency range is of no consequence as atmospheric attenuation quickly diminishes these frequency components to negligible levels. In addition, full-scale frequencies above 10 kHz are not even included in the EPNL noise metric. In fact, if the model scale data shown here were propagated out very far past the 1 ft. reference arc, the noise levels observed would be quickly attenuated and barely noticeable in the spectra. So while the 1ft. lossless data presented here exaggerate the noise of the DEN, it was valuable to evaluate the data this way so as to more closely examine this phenomenon.

Figures 19 and 20 show the spectra at nozzle azimuthal orientations of 0° and 90° for the aft polar location of 145°, a directivity angle at which jet mixing noise typically peaks. For both orientations, the DEN is quieter than both reference nozzles in the low frequency range. This is the expected result from a DEN due the mixing enhancement potential. However, it has already been pointed out that the DEN mixing characteristics were not significantly different than those from the 2D reference nozzle. In fact, above 1 kHz , the noise spectra from the DEN nearly overlays that of the 2D reference nozzle. The most significant difference is seen in the 90° azimuthal orientation plane at frequencies above 10 kHz where the airfoil self noise increases the DEN noise levels above those of the 2D reference nozzle.

It is very clear from these acoustic data in the aft angles that the acoustic suppression of the DEN suffered from the plume developing more as a single flow stream rather than as multiple smaller independent jets. The noise signature from a jet is directly related to general plume characteristics such as mixing, velocity distribution, and turbulence levels. The fact that the DEN only provided minimal noise suppression relative to the reference nozzles is entirely consistent with the flowfield measurements that showed the DEN only provided minimal mixing compared to the reference nozzles.

Conclusions

Flowfield, performance measurements and predictions and acoustic measurements were made of a DEN concept. Relative to a 2D reference nozzle, the DEN provided only minimal noise suppression in the extreme aft quadrant. The flowfield measurements and CFD simulations indicated that the individual mini-jets comprising the DEN did not mix separately, but merged into a single stream shortly downstream of the nozzle exit. As a result, the plume flowfields of the DEN and the 2D reference nozzle were very similar. Extraneous noise sources were measured from the DEN with evidence that they were associated with the array of airfoil shaped slots that formed the individual exhaust nozzles. The DEN showed a discharge coefficient approximately 4% lower than the reference nozzle and thrust losses of approximately 5% compared to the reference nozzle.

A great deal of information was gained from this work that will improve future DEN concepts. The CFD did an excellent job of predicting both the general flowfield and aerodynamic performance features of the relatively complex DEN geometry and will be an invaluable tool in the effort to minimize the performance losses in subsequent designs. There were some unexpected "lessons learned" in this work as well as a reiteration of previously known DEN challenges.

By not providing enough separation between the individual mini-jets, they quickly coalesced back into a single stream. This problem can be easily corrected by spreading the jets further apart, but will have associated performance loss issues. Based upon the CFD results shown here, the challenge of designing an array of mini-nozzles that provide the needed jet-to-jet mixing while minimizing the thrust loss is one that is well suited for the GCNS code. It is also clear that the arrangement of mini-nozzles themselves can create extraneous noise sources that must be considered. Constructive interference between the noise and flowfields of the small exhaust nozzles can generate noise that radiates to the far-field. The noise sources could be mitigated by judiciously choosing the shape and placement of the mini-nozzles. Work is continuing on improved designs using the GCNS code as a tool to evaluate the performance impact of DEN concepts with more aggressive noise reduction potential.

Acknowledgements

The authors wish to express their gratitude towards the JNL technician staff who made these measurements possible and to Dr. Ed L. Blosch for GCNS optimization and documentation.

References

[1] Schein, D.B., Hausmann, J.S., Ybarra, A.H., and Smith, D.L., "Design and Demonstration of a Flight Worthy, Very Low Jet Mixing Noise Exhaust System," Final Report, NASA Contract No. NAS3-25816, Task 16.

[2] Malone, M.B., "Turbulence Model Evaluation for Free Shear Dominated Flows," AIAA Paper No, 96-2038 presented at the 27th AIAA Fluid Dynamics Conference, June, 1996.

[3] Saiyed, N.H., Mikkelsen, K.L., and Bridges, J.E., "Acoustics and Thrust of Separate-Flow Exhaust Nozzles with Mixing Devices for High-Bypass-Ratio Engines," AIAA Paper No. 2000-1961 presented at the 6th AIAA/CEAS Aeroacoustics Conference, June, 2000.

[4] Brooks, T.F., Pope, S.D., and Marcolini, M.A., "Airfoil Self-Noise and Prediction," NASA RP-1218, 1989.

Table I Test conditions

Test Point	NPR	Tt, R
10	1.45	922
11	1.55	942
12	1.64	961
13	1.72	977
14	1.81	995

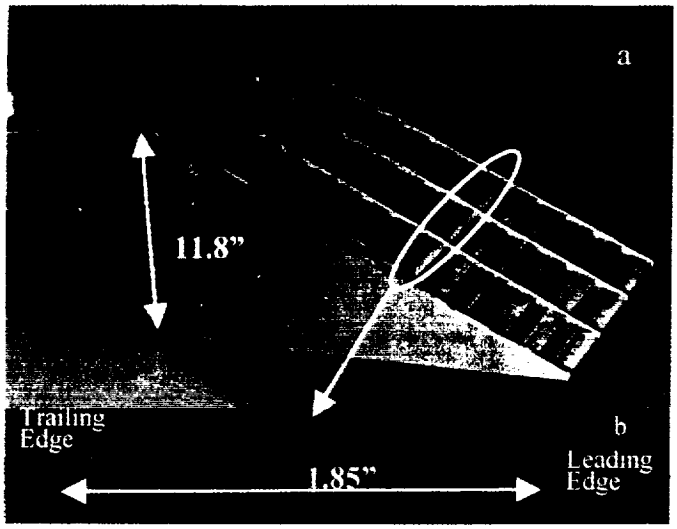

Fig. 1 Photograph of DEN a) nozzle, b) cross-section of airfoil slat.

Fig. 2 DEN installed in NASA Langley's LSAWT.

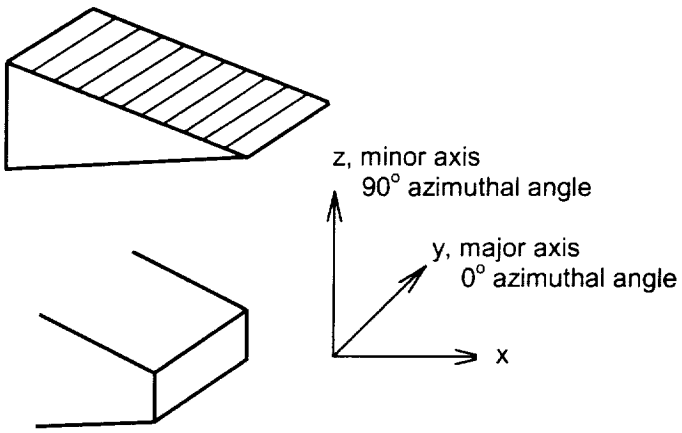

Fig. 3 Sketch of nozzle coordinate system and azimuthal orientation planes.

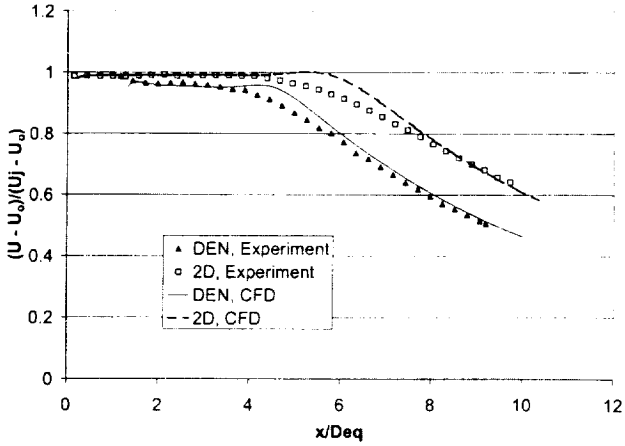

Fig. 4 Centerline velocity distribution and CFD prediction of 2D and DEN at TP 13.

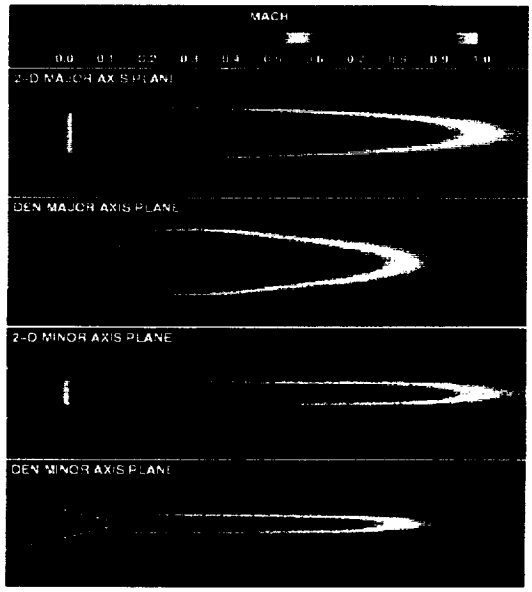

Fig. 5 CFD Mach number prediction of jet plumes for the DEN and 2D nozzles at TP 13.

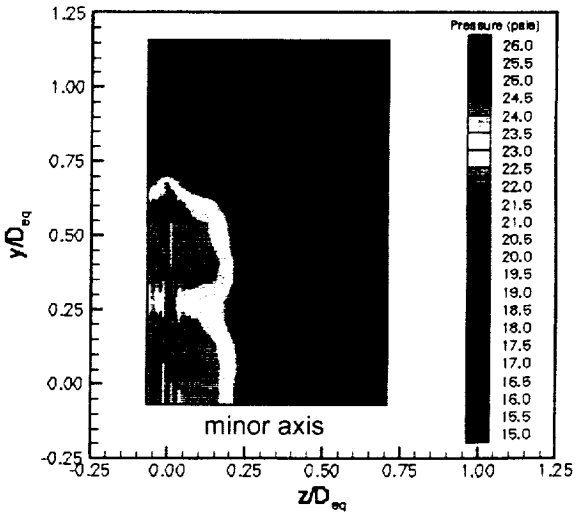

Fig. 6 Measured total pressure profile over a quadrant of the DEN at x/Deq = 0.14 at TP 13.

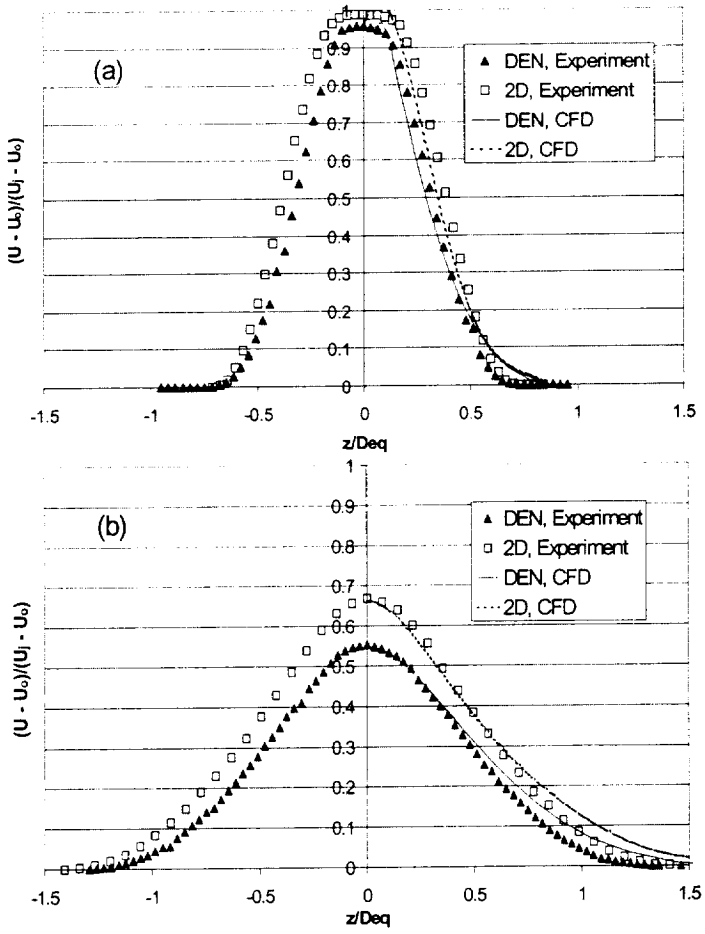

Fig. 7 Velocity profiles of the DEN and 2D nozzles in the minor axis plane at TP 13. a) DEN, x/D_{eq} = 2.61; 2D x/D_{eq} = 3.10; b) DEN, x/D_{eq} = 8.72; 2D x/D_{eq} = 9.30.

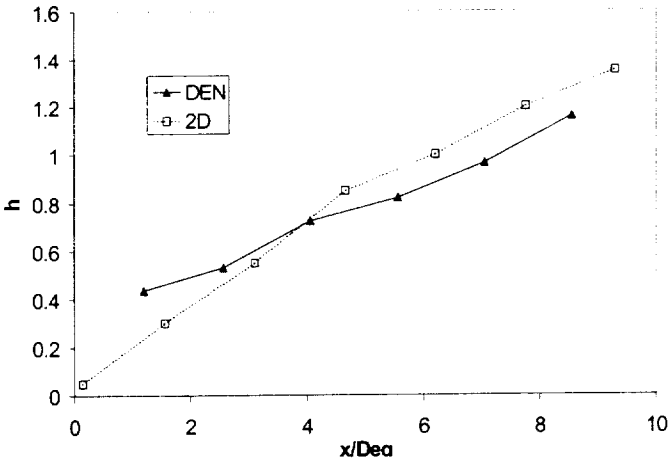

Fig. 8 Shear layer growth rates of DEN and 2D nozzles at TP 13.

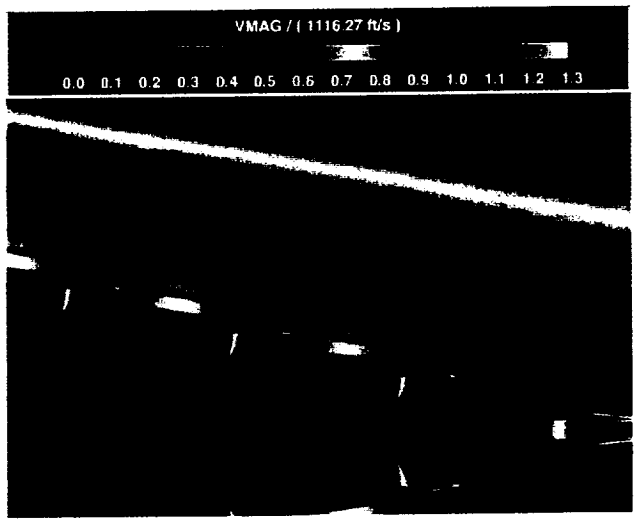

Fig. 9 CFD predictions of the velocity magnitude at the aft end of the DEN for TP 13.

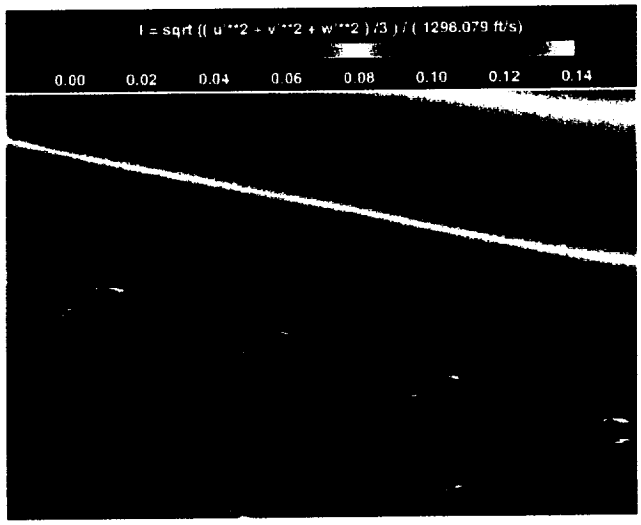

Fig. 10 CFD predictions of the turbulence intensity at the aft end of the DEN for TP13.

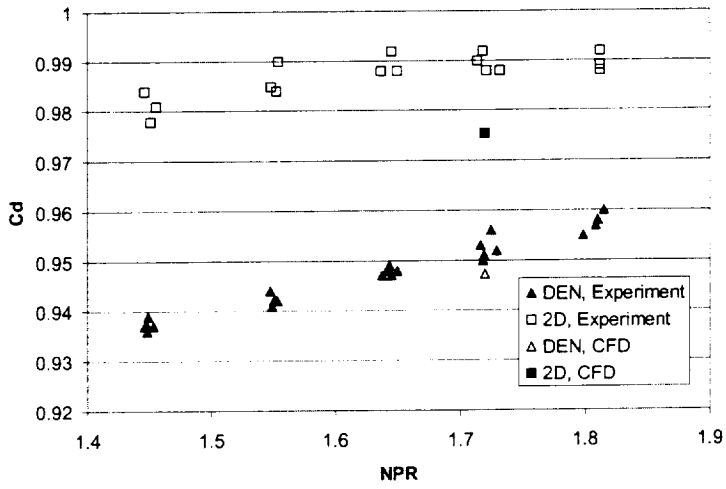

Fig. 11 Measured and predicted discharge coefficients for the DEN and 2D reference nozzle.

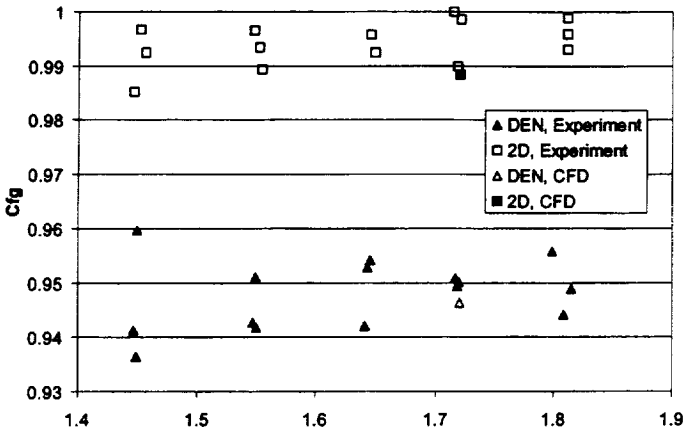

Fig. 12 Measured and predicted thrust coefficient for the DEN and 2D reference nozzles.

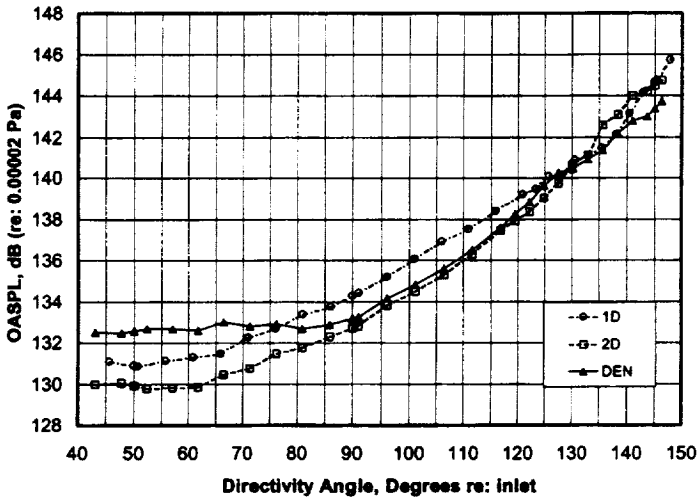

Fig. 13 OASPL for DEN and reference nozzles in the 0 degree orientation plane at TP 13.

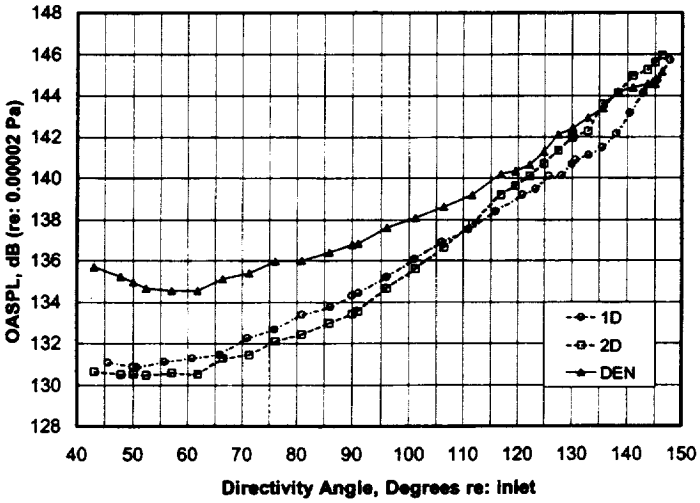

Fig. 14 OASPL for DEN and reference nozzles in the 90 degree orientation plane at TP 13.

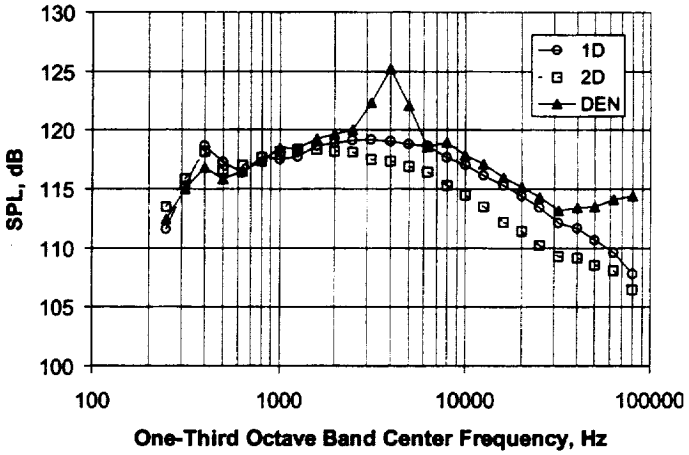

Fig. 15 1/3 octave spectra for DEN and reference nozzles in the 0 degree orientation plane at a polar angle of 50 degrees for TP 13.

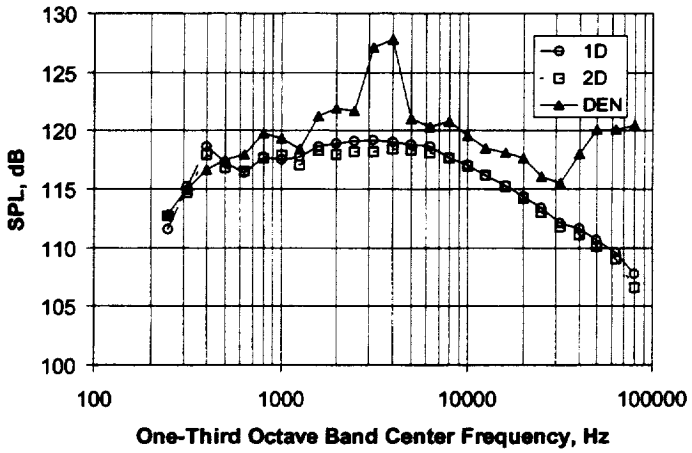

Fig 16 1/3 octave spectra for DEN and reference nozzles in the 90 degree orientation plane at a polar angle of 50 degrees for TP 13.

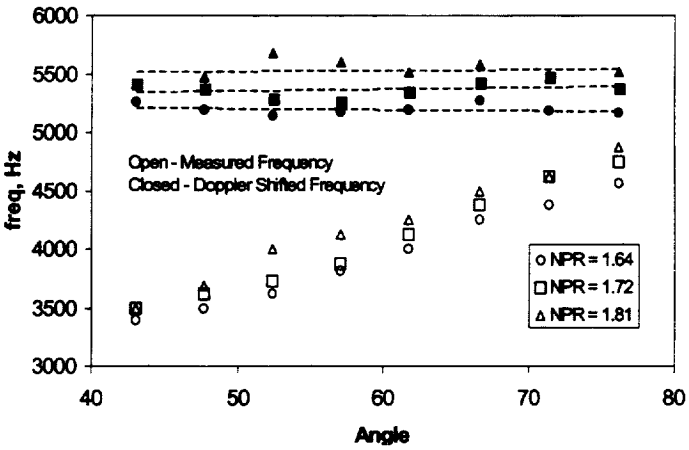

Fig. 17 Measured and Doppler corrected frequencies for the DEN assuming $M_c = 0.49$.

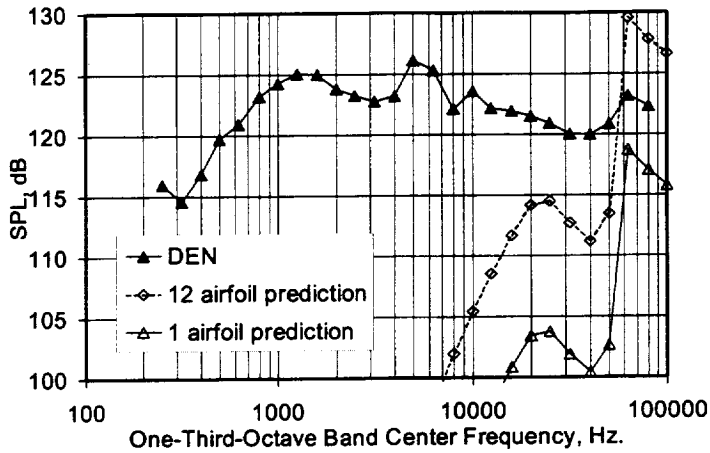

Fig. 18 Measured DEN spectra and airfoil prediction of Brooks et al.[4] at a polar angle of 90° and azimuthal angle of 90° for TP 13.

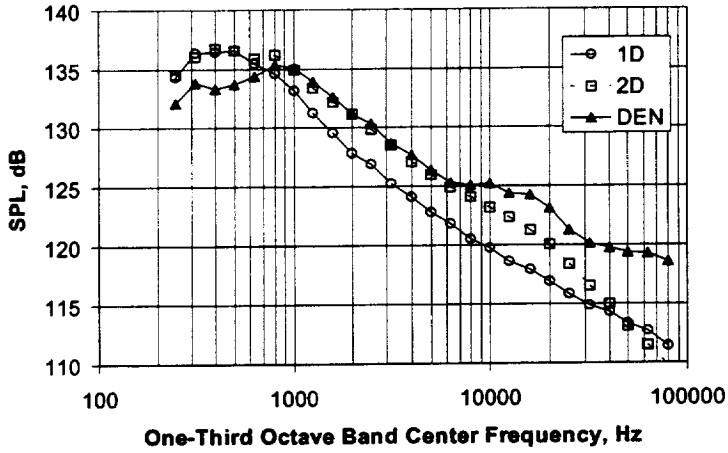

Fig. 19 1/3 octave spectra for DEN and reference nozzles in the 0 degree orientation plane at a polar angle of 145 degrees for TP 13.

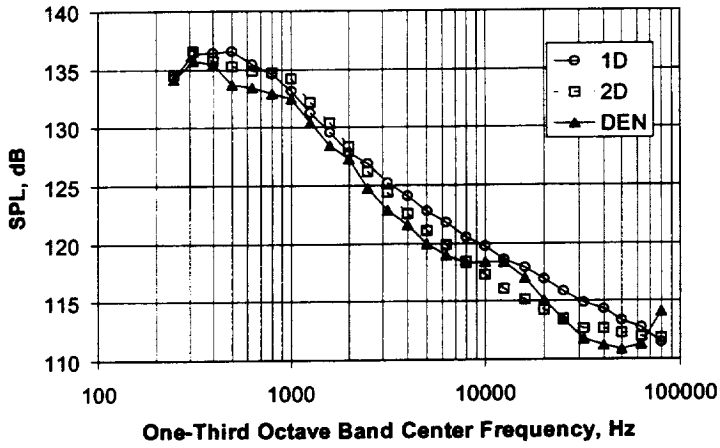

Fig. 20 1/3 octave spectra for DEN and reference nozzles in the 90 degree orientation plane at a polar angle of 145 degrees for TP 13.